Rev. Roum. Sci. Techn.– Électrotechn. et Énerg.
Vol. **71**, *2*, pp. 275–280, Bucarest, 2026

GRAPHENE PATCH ANTENNAS FOR SATELLITE RADAR: SUBSTRATE AND CHEMICAL POTENTIAL ANALYSIS

MOHAMMED ZAKARYA BABA-AHMED[1], RAHMA DJAOUDA TALEB[2], MOHAMMED AMIN RABAH[3], ASMA BEKHTI[4], RANIA MERZOUK[5]

Keywords: Patch antennas; Radar satellite communication; Antenna arrays; X-band frequencies; Design optimization; Graphene.

This paper presents the design, simulation, and experimental validation of high-performance rectangular patch antennas and their arrays specifically designed for X-band radar applications. CST Microwave Studio was used to enhance the antenna designs, maximizing radiation efficiency and achieving optimal performance at 10 GHz with the appropriate impedance. Rogers RT5880 outperformed FR-4 across gain, reflection coefficient, and voltage standing wave ratio (VSWR) when compared with two substrates. The work culminated in the development of a four-element antenna array, achieving a remarkable gain of 11.82 dBi. The experimental measurements prove the validity of the simulated results, confirming that this design is viable and can be used in advanced satellite communications. Graphene is also explored as a conducting material due to its tunable electrical properties by chemical potential variations, and its performance is compared with that of conventional copper. All these novel improvements contribute to the development of next-generation reconfigurable antennas that offer greater flexibility and performance for high-quality satellite radar communication.

1. INTRODUCTION

The continuous expansion of satellite communication and radar systems has led to an increasing demand for compact, high-performance antenna arrays capable of operating in the X-band while maintaining stable radiation characteristics and design flexibility. Printed patch antennas remain a widely adopted solution due to their low-profile structure, ease of fabrication, and compatibility with planar and array configurations [1,2]. Despite these advantages, conventional patch antenna arrays often suffer from limited adaptability and restricted reconfiguration capabilities when deployed in dynamic satellite environments [3,4].

Starting from a single patch antenna, it comes to the four-element array designed for satellite radar systems operating at 9.4 GHz [5,6]. The system with Tx/Rx antennas, reflectors, absorbers, and a tuning strip provides high gain, precise beamforming, and minimal interference, constituting a compact and efficient solution validated experimentally in Fig. 1 [7].

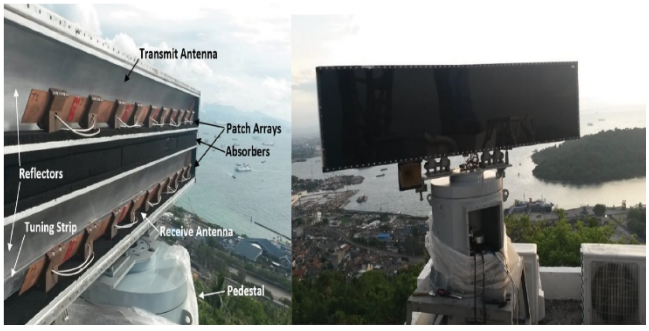

Fig. 1 – Example of an experimental setup of the X-band patch antenna system for satellite radar applications [7].

Among these materials, graphene has attracted significant attention due to its high electrical conductivity and its chemical potential, which can be controlled through external biasing. These properties enable continuous frequency tuning without modifying the antenna geometry or introducing additional lumped switching elements, making graphene a promising candidate for adaptive X-band antenna applications [8,9].

In this work, a four-element X-band patch antenna array designed on a Rogers substrate is presented for satellite radar applications. The antenna array is designed and optimized using CST Microwave Studio, and its performance is evaluated in terms of impedance matching and radiation characteristics, demonstrating a compact and efficient configuration suitable for high-frequency satellite systems. In addition, a comparative study is conducted to assess the impact of graphene-based tunability by varying the chemical potential of the graphene patch, providing practical insight into performance evolution under controlled reconfiguration.

The main contribution of this paper lies in the integration of graphene into an X-band patch antenna array and in the systematic evaluation of its reconfigurable behavior under realistic substrate conditions. The presented results highlight the influence of material properties on antenna performance and offer useful guidelines for the design of adaptive antenna arrays for future satellite communication and radar systems.

2. DESIGN OF THE PATCH ANTENNA FOR RADAR APPLICATIONS IN THE X-BAND

2.1 GEOMETRY OF THE SIMULATED ANTENNA

Table 1

Parametric equations for a rectangular patch antenna.

Antenna Parameters	Equations
Actual patch length	$L_p = L_{eff} - 2\Delta l$ (1)
Effective length	$L_{eff} = \frac{c}{(2f_r\sqrt{\varepsilon_{r,eff}})}$ (2)
Length extension	$\Delta l = \frac{\left(0.412h(\varepsilon_{r,eff}+0.3)(w/h+0.264)\right)}{\left((\varepsilon_{r,eff}-0.258)(w/h+0.8)\right)}$ (3)
Dielectric constant	$\varepsilon_{r,eff} = \frac{(\varepsilon_r+1)}{2} + \frac{(\varepsilon_r-1)}{2}\left[1+12\frac{h}{w}\right]^{-1/2}$ (4)
Patch width	$W_p = \frac{c}{(2f_r\sqrt{(\varepsilon_r+1)})}$ (5)
Substrate length	$L_s = L_p + 6h$ (6)
Substrate width	$W_s = L_s + 6h$ (7)
Line width	$W_f = \frac{8e^A}{e^{2A-2}} \times h$ (8)
	with
	$A = \frac{Z\sqrt{(2(\varepsilon_r+1)}}{120} + \frac{1}{2} + \frac{(\varepsilon_r-1)}{(\varepsilon_r+1)} + \left(h\ln\frac{\pi}{2} + \frac{1}{\varepsilon_r} \times \ln\frac{4}{\pi}\right)$

The antenna under study is a rectangular patch antenna

[1,2,3,4,5] Department of Telecommunication, Faculty of Technology, University of Abou-Bekr Belkaid of Tlemcen, Laboratory of Telecommunication of Tlemcen (LTT), Tlemcen, Algeria.
[1,3] Faculty of Technology of the University of Hassiba Ben Bouali of Chlef, Chlef, Algeria.
E-mails: mohammedzakarya.baba-ahmed@univ-tlemcen.dz, rahmadjaouda.taleb@univ-tlemcen.dz, mohammedamin.rabah@univ-tlemcen.dz, asma.bekhti@univ-tlemcen.dz, rania.merzouk@univ-tlemcen.dz

DOI: 10.59277/RRST-EE.2026.2.18

operating at a frequency of 10 GHz, matched to an input impedance of 50 Ω, and fabricated using two types of substrates:

- FR-4 (Lossy): with a relative permittivity of $\varepsilon_r = 4.3$ and a thickness of $h = 1.6$ mm [10].
- Rogers RT5880: with a relative permittivity of $\varepsilon_r = 2.2$ and a thickness of $h = 0.8$ mm [11].

The ground plane is made of the same material as the patch (copper) and has a thickness of $t = 0.035$ mm.

The dimensions of the antenna were calculated using the equations [12–14] provided in Table 1.

The results after calculations are stated in Table 2.

Table 2

Dimensions of the proposed rectangular patch antenna.

Parameters [mm]	W_g	L_g	W_p	L_p	W_a	L_a	h	t
FR-4 (LOSSY)	18.81	16.10	9.208	6.499	3.11	4.80	1.6	0.035
Rogers RT5880	16.66	14.45	11.85	9.651	2.48	2.40	0.8	0.035

2.2 ADAPTATION AND OPTIMIZATION

At this stage, modifications were made by incorporating notches with a width of $Gpf = 0.4$ mm and a length of $Fi = 1.9816$ mm for FR-4, and Gpf = 0.1 mm and a length of $Fi = 3.36$ mm for Rogers. Additionally, the width of the patch was increased based on a parametric study conducted using the software, resulting in a patch width of $Wp = 11$ mm for FR-4 and $Wp = 14.2$ mm for Rogers, to ensure matching at the desired frequency [15] of 10 GHz. This configuration is illustrated in Fig. 2.

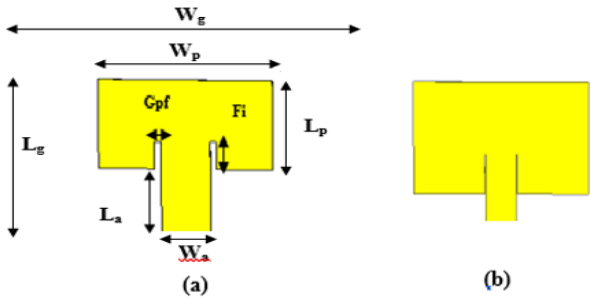

Fig. 2 – Structure of the patch antenna with notches. (a) FR-4, (b) Rogers.

2.3 REFLECTION COEFFICIENT S_{11}

Figure 3 presents the reflection coefficient S_{11} of the antenna. At the desired resonance frequency of 10 GHz, an S_{11} value of -17.22 dB is observed for FR-4, while a superior performance of -21.22 dB is achieved with Rogers, demonstrating more effective impedance matching to the load. These results highlight that the adjustments made successfully achieved the desired frequency, with more favorable outcomes for Rogers.

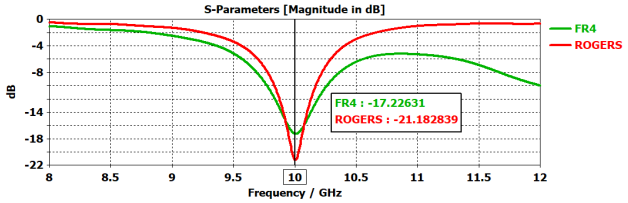

Fig. 3 – Reflection coefficient of the patch antenna with notches.

2.4 NEW ANTENNA STRUCTURE

At this stage, a new structure is introduced by incorporating various cuts of different shapes. The new configuration features rectangular slots and symmetrical notches, along with a central slot and curved edges at the extremities, as illustrated in Fig. 4.

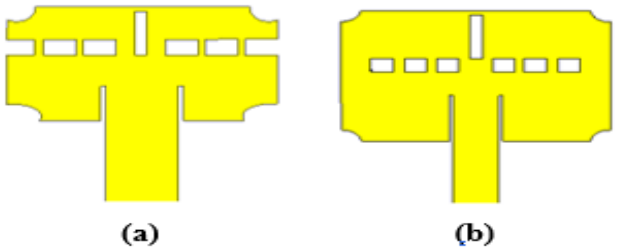

Fig. 4 – New antenna structure. (a) FR-4, (b) Rogers.

2.5 REFLECTION COEFFICIENT S_{11}

Figure 5 presents the reflection coefficient S_{11} of the antennas using FR-4 and Rogers substrates. The results show that the antenna is perfectly tuned to the targeted resonance frequency of 10 GHz. For the FR-4 substrate, the S_{11} value reaches -21.66 dB, indicating good impedance matching. However, the Rogers substrate exhibits even better performance, achieving an S_{11} of -29.25 dB, demonstrating more effective impedance matching and lower return loss. These results emphasize the positive impact of using the Rogers substrate on the antenna's performance at the resonance frequency of 10 GHz.

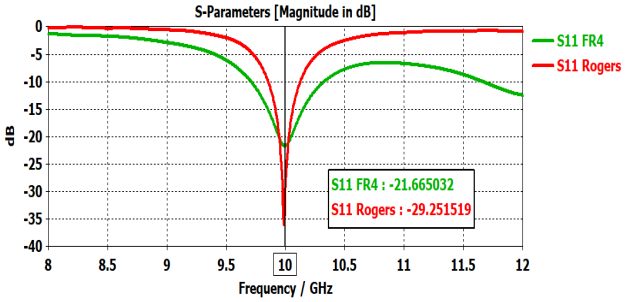

Fig. 5 – Reflection coefficient of the new antenna structure with FR-4 and Rogers substrates.

2.6 GAIN

Figure 6 illustrates the variation of gain as a function of frequency. At the frequency of 10 GHz, a gain of 2.07 dBi is achieved with the FR-4 substrate, while the Rogers substrate significantly outperforms it, achieving a gain of 7.42 dBi. These results highlight the superior performance of the Rogers substrate in terms of gain, which could be crucial for satellite applications requiring enhanced efficiency and extended signal range.

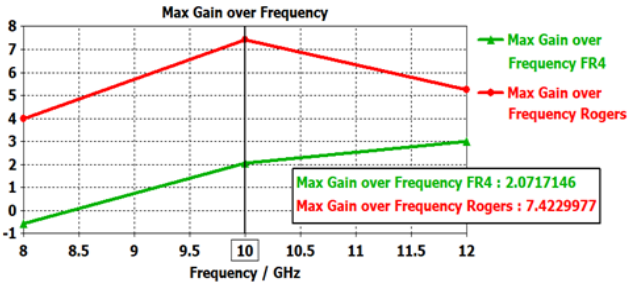

Fig. 6 – Gain of the new structure with FR-4 and Rogers substrates.

2.7 VOLTAGE STANDING WAVE RADIO VSWR

As shown in Fig. 7, the voltage standing wave ratio (VSWR) remains below 2 for the FR-4 substrate, while it is even lower for the Rogers substrate. This indicates better impedance matching between the antenna and the feed line at the desired resonance frequency when using Rogers.

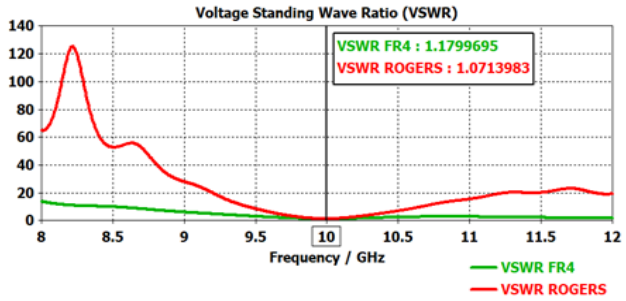

Fig. 7 – Voltage Standing Wave Ratio (VSWR) of the new structure with FR-4 and Rogers substrates.

Table 3 presents a detailed comparison of the performance of the FR4 and Rogers substrates in terms of three key parameters: the S_{11}, gain, and VSWR.

Table 3

Comparison of FR4 and Rogers results

Parameters	S_{11}	Gain	VSWR
FR4	-21.66	2.07	1.17
Rogers	-29.25	7.42	1.07

When comparing the performance between FR4 and Rogers, Rogers provides significantly superior results. The low value of S_{11} and high gain for Rogers as compared to FR4 prove better impedance matching and higher efficiency for the antenna. For Rogers, the S_{11} is -29.25 dB with a gain of 7.42 dBi and a VSWR of 1.07, whereas for FR4, the S_{11} is -21.66 dB with a gain of 2.07 dBi and a VSWR of 1.17. We will certainly choose Rogers as the material of choice to continue our work and to build the array based on these undisputed results. The selection of Rogers was based on the low tangent loss, excellent dimensional stability, and advanced dielectric properties that characterize this material.

3. ANTENNA ARRAY DESIGN

Increasing the number of radiating elements can permit improvements in both gain and matching, which is why we are considering designing an antenna array.

3.1 FOUR-ELEMENT PARALLEL ARRAY

For better performance and to achieve the desired frequency of 10 GHz, a four-element parallel array has been designed. The configuration of this array is shown in Fig. 8. The goal with this structure is to enhance the matching compared with a two-element array and increase the gain.

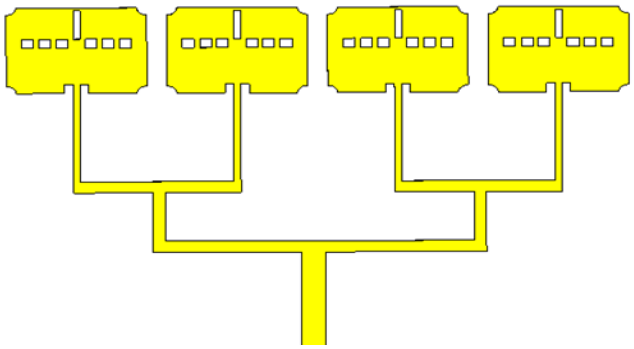

Fig. 8 – The four-element parallel array's structure.

3.2 REFLECTION COEFFICIENT S_{11}

The four-element array's reflection coefficient of -23.42 dB and our resonant frequency of 10 GHz are a perfect match.

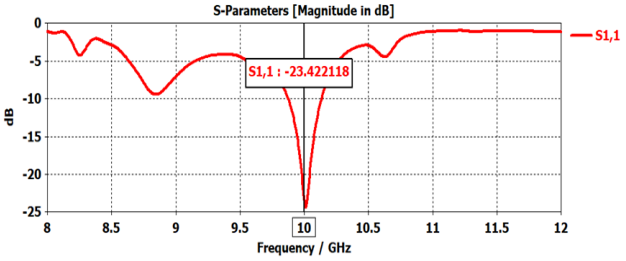

Fig. 9 – S_{11} of the four-element array.

3.3 GAIN

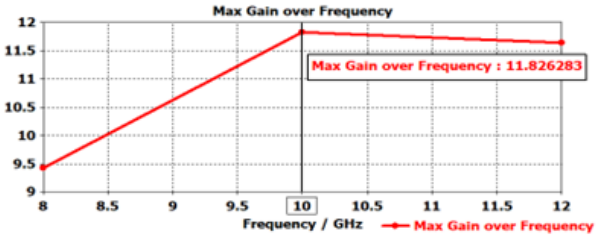

Fig. 10 – The four-element array's gain.

For our application, the gain of 11.82 dBi at 10 GHz is perfect. These exceptional performance outcomes have greatly pleased us.

3.3 VOLTAGE STANDING WAVE RADIO VSWR

From the Fig. 11, we see that 1.14 is the VSWR. This value, which is less than 2, shows that the antenna is suitable for the desired frequency.

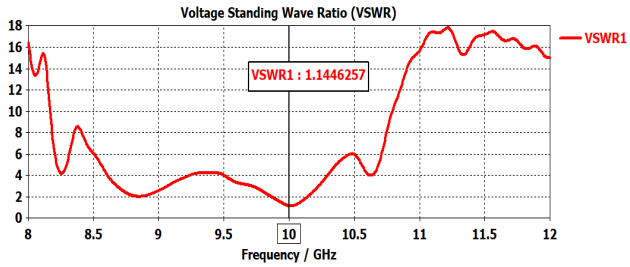

Fig. 11 – The four-element array's VSWR.

The simulation of a four-element antenna array produced excellent results. We achieved remarkable matching and gains, confirming the efficiency and performance of our design.

4. EXPERIMENTAL VALIDATION

4.1 IMPLEMENTATION OF THE FOUR-ELEMENT ANTENNA ARRAY

Figure 12 shows the implementation of the antenna array, consisting of copper metallization and a Rogers RT5880 substrate of a four-element array with dimensions of 65x44 mm. The fabrication of the antenna array was carried out at ALMITech SNC in Kouba, Algiers.

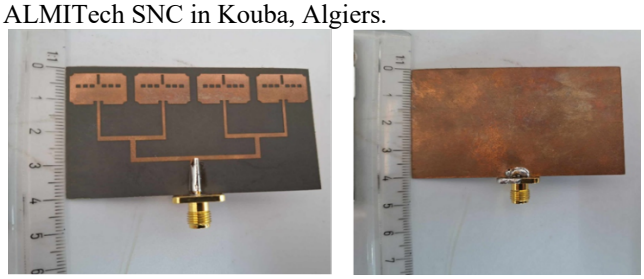

Fig. 12 – Implementation of the four-element antenna array based on Rogers RT5880 at ALMITech.

4.2 MEASUREMENT OF REFLECTION COEFFICIENT AND VOLTAGE STANDING WAVE RATIO

Figure 13 shows the experimental setup used to measure the performance of the antenna array. It is connected to a network analyzer to evaluate its characteristics, such as the reflection coefficient and VSWR. The measurements were carried out at the Signal Processing Laboratory [16] at the University of Sidi Bel Abbès in ALGERIA.

Fig. 13 – Testing of the four-element antenna array.

Following the calibration of the network analyzer in the frequency range between 8 GHz and 12 GHz, the obtained results are as follows.

REFLECTION COEFFICIENT

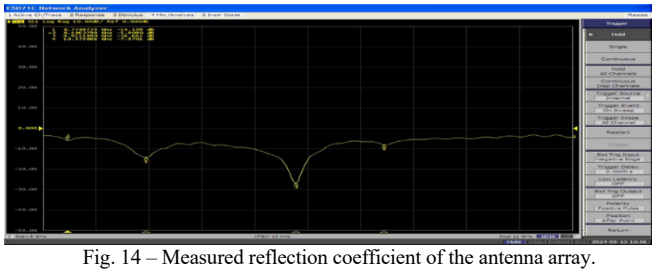

Fig. 14 – Measured reflection coefficient of the antenna array.

VSWR

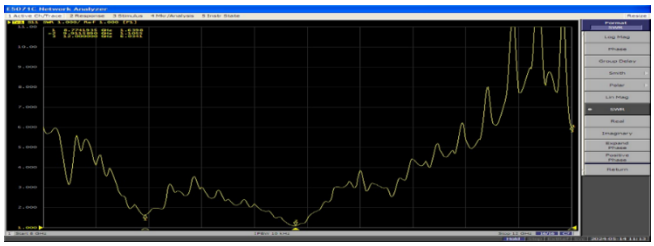

Fig. 15 – Voltage standing wave ratio (VSWR) of the antenna array.

After exporting the results from the network analyzer, we compared them with the results from the electromagnetic simulations. The comparison between the simulations and the measurements for the antenna array is presented in Fig. 16.

Both curves show good agreement, with a slight difference at the resonant frequency. The simulation presents a resonant frequency of 10 GHz, while the implementation shows a resonant frequency of 9.91 GHz.

The simulation also shows a minimum value of -23.42 dB for S_{11}, while the implementation shows a minimum value of -26.66 dB.

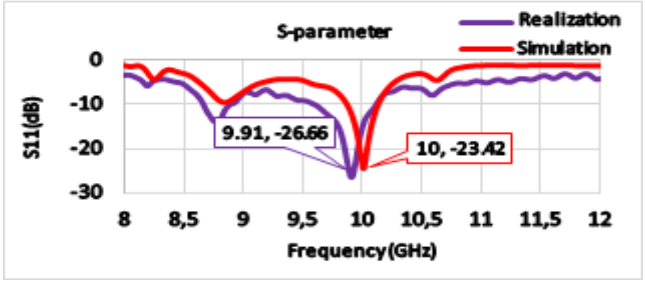

Fig. 16 – Comparison between the simulated and measured reflection coefficients of the antenna array.

This difference may be attributed to variations in the properties of the real materials compared to the idealized simulation assumptions, as well as potential discrepancies during the fabrication and measurement process.

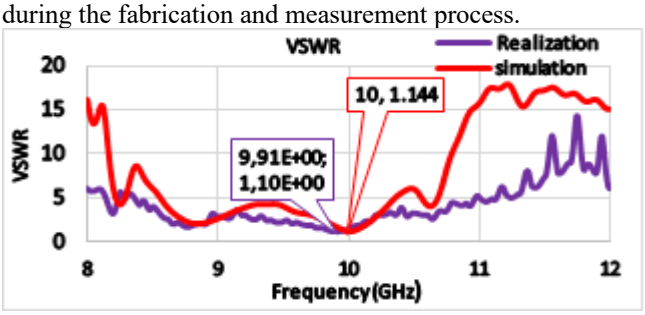

Fig. 17 – Comparison of the simulated and measured VSWR of the antenna array.

Figure 17 shows the VSWR as a function of frequency. It contrasts the simulation and the measured outcomes. The numbers shown in Fig. 28 indicate that the measurement's minimum VSWR is roughly 1.1 at 9.91 GHz, whereas the simulation's minimum is roughly 1.144 at 10 GHz. There are clear differences between the simulation and the implementation in the shapes of the two curves.

The implementation displays 9.91 GHz, whereas the simulation displays a resonant frequency of 10 GHz. Additionally, the implementation displays a minimum S_{11} value of -26.66 dB, while the simulation shows -23.42 dB. These variations are probably caused by discrepancies between the properties of real materials and the idealized assumptions in the simulation, as well as possible differences during the fabrication and measurement processes [17]. Comparably, the VSWR comparison shows a minimum value of roughly 1.144 at 10 GHz in the simulation and 1.1 at 9.91 GHz in the measurements, with discernible variations in the shapes of the curves.

5. COMPARISON WITH RECENT WORKS

The performance characteristics of the suggested antenna and those documented in earlier research are compared in Table 4, which summarizes the performance metrics of different antennas operating within the X-band, while focusing on the reflection coefficient (S_{11}), maximum gain, and VSWR.

Table 4

A comparison of the suggested antenna and some published studies.

References	X-Bande Frequency (GHz)	S_{11} (dB)	Gain (dBi)	VSWR
[18]	10.1	-15	7.2	/
[19]	9.7	-26.5	5	/
[20]	10,82	-28	4.01	1.08
[21]	8.49	−25.78	6.98	/
Our work	10 (Antenna)	-29.25	7.42	1.07
	10 (Antenna Array)	-23.42	11.82	1.14

It can be observed from the references that they have depicted different results: [18] achieved a reflection coefficient of -15 dB with a gain of 7.2 dBi at 10.1 GHz, and [19], on the other hand, documents an improved S_{11} of -26.5 dB, while recording a gain of 5 dBi at 9.7 GHz. Reference [20] has demonstrated remarkable results at 10.82 GHz with S_{11} equal to -28 dB, a gain of 4.01 dBi, and a VSWR of 1.08.

By contrast, our suggested design shows an excellent balance of performance metrics at 10 GHz, with a VSWR of 1.14, an exceptionally high gain of 11.82 dBi, and a reflection coefficient of -23.42 dB. These outcomes

demonstrate our design's superior capabilities for X-band applications, particularly in obtaining high gain with minimal reflection and ideal VSWR. This advancement highlights the potential of the proposed antenna for high-performance satellite communication systems.

6. RECONFIGURABILITY WITH GRAPHENE MATERIAL

In this section, we will investigate an additional method for reconfigurability using graphene as an agile material. To put this strategy into practice, graphene will be used in place of copper. Graphene has a high electrical conductivity and can change its chemical potential, which allows for real-time adjustment of its radiative properties. For dynamic frequency tuning and beam control, graphene antennas are especially well-suited [3].

The resonant frequency shifts noticeably when the patch material is changed from copper to graphene; copper resonates slightly below 10 GHz, while graphene shifts it slightly above 10 GHz. Although graphene has a larger bandwidth, both materials show notable dips in the S-parameter magnitude at their respective resonant frequencies, indicating effective impedance matching. This change in resonant frequency through material modification illustrates a straightforward technique for patch antenna reconfigurability. Graphene's high carrier mobility and tunability shift the resonant frequency above 10 GHz, offering more design flexibility, while copper's well-known stability and high conductivity provide a resonant frequency at 10 GHz. Furthermore, as shown in Fig. 18, graphene's unique properties enable dynamic reconfigurability via external stimuli, such as chemical doping or electric fields, enabling real-time tuning of the resonant frequency.

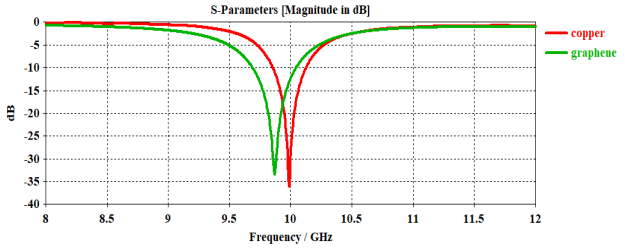

Fig. 18 – Comparison of S-parameters for copper and graphene.

Figure 19 illustrates how copper and graphene have different maximum gains over frequency. Over the entire frequency range, copper exhibits higher gain, peaking at 7.5 dB around 10 GHz. Despite having a lower gain, graphene offers wider bandwidth capabilities and a respectable peak gain of 5.5 dB. This comparison highlights the trade-offs between using copper and graphene for satellite radio frequency and microwave systems, where the choice of material depends on requirements for gain, bandwidth, and other material properties.

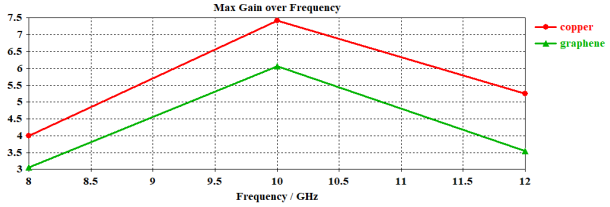

Fig. 19 – Gain comparison between graphene and copper.

6.1 GRAPHENE WITH VARYING CHEMICAL POTENTIALS

Graphene's RF and microwave performance can be dynamically adjusted by changing its chemical potential, which makes it ideal for reconfigurable satellite applications. To show how this tunability can be used to maximize performance in satellite communication systems, this study examines the effects of graphene's chemical potential from 0 to 4 eV on its reflection coefficient (S_{11}), VSWR, and gain.

Figure 20 illustrates how the reflection coefficient (S_{11}) varies for graphene with various chemical potentials, particularly for satellite applications. Graphene's S-parameters can be dynamically adjusted by changing the chemical potential. This offers a potent way to achieve reconfigurability, enabling real-time optimization of performance. The resonant frequency stays constant at about 9.88 GHz as the chemical potential increases, but the S_{11} dip varies. The S_{11} values are higher at lower chemical potentials (0 and 0.5 eV), indicating less effective impedance matching. On the other hand, the S_{11} dips become more noticeable at higher chemical potentials (between 1 and 4 eV), with the biggest dip happening at a chemical potential of 1.5 eV, indicating improved impedance matching efficiency.

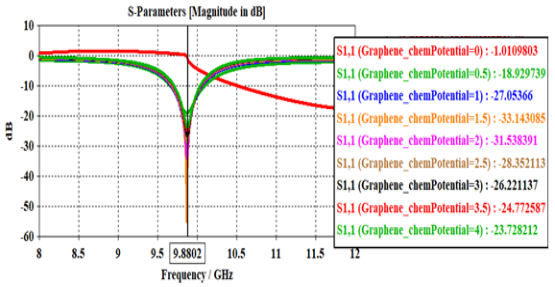

Fig. 20 – The impact of chemical potential on graphene antenna S-parameters.

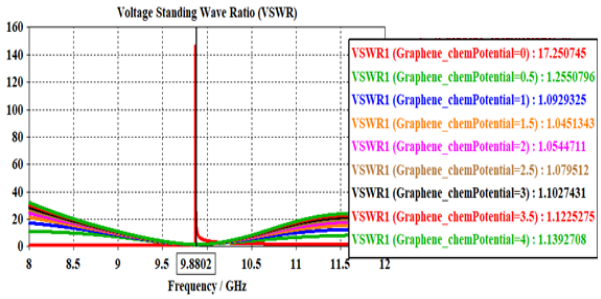

Fig. 21 – Effect of chemical potential on the VSWR of graphene antenna.

Figure 21 shows how changing graphene's chemical potential significantly affects its VSWR at various frequencies. Graphene's suitability for dynamic reconfigurability in satellite communication systems is highlighted by higher chemical potentials, which result in improved impedance matching and lower VSWR values.

Figure 22 shows graphene's maximum gain over frequency at various chemical potentials between 0 and 4 eV. Graphene maintains a comparatively high gain throughout the frequency range, with a peak gain of 6.585 dB at 9.8802 GHz at a chemical potential of 0. The maximum gain fluctuates significantly around the resonant frequency as the chemical potential rises. A lower peak gain of 3.709 dB is obtained with a chemical potential of 0.5 eV. Nevertheless, the gain typically rises with increasing chemical potentials; at a chemical potential of 4 eV, it reaches 6.473 dB. Graphene can be used to improve signal strength and quality in satellite communication systems because of its tunability, which

enables the optimization of gain performance.

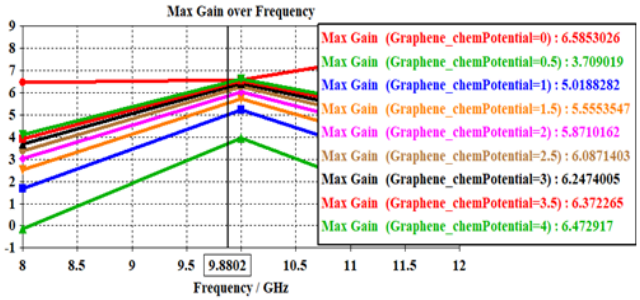

Fig. 22 – The impact of chemical potential on graphene antenna gain.

7. CONCLUSION

For X-band radar satellite applications, this study effectively designed, simulated, and experimentally verified high-performance rectangular patch antennas and arrays. At 10 GHz, ideal impedance matching and radiation efficiency were attained using CST Microwave Studio. The superiority of Rogers RT5880 substrates over FR-4 substrates was confirmed by a comparative analysis, which allowed for a high gain of 11.82 dBi with the four-element array.

The robustness of the suggested designs was confirmed by the strong agreement between simulation and measurement results. Furthermore, S_{11}, VSWR, and gain were greatly affected by adjusting graphene's chemical potential, indicating its potential in reconfigurable satellite antennas. These results offer a solid foundation for upcoming advancements in advanced satellite communication systems' materials and design approaches.

ACKNOWLEDGMENT

The authors express their gratitude to the University of Sidi Bel Abbès's Signal Processing Laboratory for providing the Agilent PNA (Network Analyzer) used in their experiments.

CREDIT AUTHORSHIP CONTRIBUTION STATEMENT

AHMED MOHAMMED ZAKARYA BABA: Writing – conceptualization.
RAHMA DJAOUDA TALEB: Formal analysis and investigation.
MOHAMMED AMIN RABAH: Methodology.
ASMA BEKHTI: Writing - original draft preparation.
RANIA MERZOUK: Review and editing.

Received on 15 May 2025

REFERENCES

1. A. Aloman, G. Miguel-Poveda, I. Nicolaescu, F. Popescu, L. Buzincu, *Circularly polarized periodic leaky-wave antenna based on a coaxial line with helical slot*, Rev. Roum. Sci. Techn. – Électrotechn. et Énerg., **70**, *1*, pp. 87–90 (2025).
2. M.Z. Baba-Ahmed, R.D. Taleb, M.A. Rabah, S. Benabbou, M.I. Soufi, *Hybrid design patch antenna for X-band satellite communication*, Rev. Roum. Sci. Techn. – Électrotechn. et Énerg., **70**, *3*, pp. 379–384 (2025).
3. B. Mishra, A.K. Singh, T.Y. Satheesha, R.K. Verma, V. Singh, *From Past to Present: A Comprehensive Review of Antenna Technology in Modern Wireless Communication*, Journal of Engineering Science & Technology Review, **17**, *3*, pp. 1–10 (2024).
4. R.D. Taleb, M.Z. Baba-Ahmed, M.A. Rabah, *Reconfigurable graphene antenna for a network cognitive radio: A novel solution for X-band satellite communications*, Advances in Space Research, **73**, *9*, pp. 4742–4750 (2024).
5. Z. Patel, A. Sarvaiya, *A novel compact RHCP antenna with wide 3 dB AR bandwidth for S-band IRNSS application*, 2023 International Conference on Device Intelligence, Computing and Communication Technologies (DICCT), pp. 416–421 (2023).
6. R.D. Taleb, M.Z. Baba-Ahmed, F. Bousalah, M.A. Rabah, *Reconfigurable and ecological intelligent antenna for satellite communication*, Proc. Int. Conf. on Artificial Intelligence in Renewable Energetic Systems, pp. 183–188 (2022).
7. A.A. Lestari, L.P. Ligthart, *FMCW radar antenna using a half parabolic reflector with microstrip-patch-array offset feed and tuning strip*, Journal of Electromagnetic Waves and Applications, **35**, *3*, pp. 400–415 (2021).
8. Z. Jin, Y. Rong, J. Yu, F. Wu, *Design of a compound reconfigurable terahertz antenna based on graphene*, Plasmonics, **19**, *2*, pp. 621–629 (2024).
9. S.N.H. Sa'don, M.H. Jamaluddin, A. Althuwayb, B. Alali, *A review: The influence of graphene material integration in antenna characteristics in the presence of bias for fifth and sixth generation wireless communication application*, Nano Communication Networks, **39**, pp. 1–10 (2024).
10. S.C. Petchetty, K.H. Murali, S.R. Kumbha, *A low-profile wideband triple-layer reflectarray unit cell for X-band applications*, Proc. 2023 First Int. Conf. on Microwave, Antenna and Communication (MAC), pp. 1–4 (2023).
11. R. Gopalan, G. Nareshkannan, A. Pooja, K. Karthik, S. Pavithra, Y. Mohan Sundar, *Design and performance analysis of a microstrip patch antenna for next-generation wireless networks using 4.9 GHz*, 2025 7th International Conference on Inventive Material Science and Applications (ICIMA), pp. 78–84 (2025).
12. R.D. Taleb, M.Z. Baba-Ahmed, M.A. Rabah, *Design of reconfigurable antennas with advanced techniques for satellite radar communication systems*, Electrotehnică, Electronică, Automatică (EEA), **73**, *4*, pp. 80–87 (2025).
13. H.M. Marhoon, H.A. Abdulnabi, Y.Y. Al-Aboosi, *Designing and analyzing of a modified rectangular microstrip patch antenna for microwave applications*, Journal of Communications, **17**, *8*, pp. 668–674 (2022).
14. F.A. Ningrum, S. Muliyani, F. Fadjrianah, M.R. Effendi, A. Munir, *Proximity-coupled Ku-band patch array antenna for imaging application*, Proc. 2022 IEEE Int. RF and Microwave Conference (RFM), Penang, Malaysia, pp. 1–5 (2022).
15. M.S. Shakhirul, M. Jusoh, Y.S. Lee, C.N. Husna, *A review of reconfigurable frequency switching technique on microstrip antenna*, Journal of Physics: Conference Series, **1019**, *1*, pp. 1–8 (2018).
16. M.C. Farah, F. Salah-Belkhodja, K. Khelil, *A design of a compact microwave diplexer in microstrip technology based on bandpass filters using stepped impedance resonator*, Journal of Microwaves, Optoelectronics and Electromagnetic Applications, **21**, *2*, pp. 242–264 (2022).
17. D. Helena, A. Ramos, T. Varum, J.N. Matos, *Antenna design using modern additive manufacturing technology: A review*, IEEE Access, **8**, pp. 177064–177083 (2020).
18. J. Jiang, Y. Li, L. Zhao, X. Liu, *Wideband MIMO directional antenna array with a simple meta-material decoupling structure for X-band applications*, The Applied Computational Electromagnetics Society Journal (ACES), pp. 556–566 (2020).
19. P. Gupta, M. Bharti, A. Kumar, *Circular polarized two-element compact dual-band MIMO antenna for 5G and wearable applications*, Rev. Roum. Sci. Techn. – Électrotechn. et Énerg., **67**, *3*, pp. 321–326 (2022).
20. B. Agrawal, R. Sharma, R.K. Khanna, *A novel design of triangular-shaped hexagonal fractal antenna for satellite communication*, International Journal of Advanced Technology and Engineering Exploration, **10**, *99*, pp. 1–10 (2023).
21. K.S. Kola, A. Chatterjee, *A high-gain and low cross-polarized printed fractal antenna for X-band wireless application*, International Journal of Communication Systems, **34**, *10*, pp. 1–10 (2021).